Charge Transfer and Ionization in Collisions between Atomic Ions and Rare-Gas Atoms for Primary-Ion Energies below 100 eV*

William B. Maier II
Los Alamos Scientific Laboratory, University of California, Los Alamos, New Mexico 87544
(Received 14 July 1971)

Cross sections for the production of Kr^+, Kr^{++}, Xe^+, and Xe^{++} in collisions of H^+, He^+, and Ne^+ with Kr and Xe have been measured for primary-ion kinetic energies E between 0.5 and 100 eV. These cross sections rise rather sharply as E is increased, reach a maximum, and then decrease rather slowly. Maximum values of the cross sections range from 0.1 to 40 $Å^2$. Production of the doubly charged ions must correspond to the production of a free electron; these ionization processes have apparent threshold energies 0–4 eV above the true threshold energies. Collisions of H^+ with Kr and Xe do not produce doubly charged positive ions. The cross sections for reactions that release a free electron are not adequately represented by any of the theoretical expressions with which the experimental data were compared. Cross sections for the production of singly charged positive ions are larger for the more complex target atoms and lighter primary ions; these cross sections are well represented by the charge-transfer theory of Rapp and Francis when the experimental cross sections are large, but not otherwise. Rapp and Francis's formulas are not applicable to charge-transfer reactions having small cross sections. The present experimental data agree fairly well with previous experimental results.

I. INTRODUCTION

The present theory of collisions between ions and neutrals is most reliable for atomic ions and neutral atoms. Rather complete treatments exist for charge transfer in atomic collisions.[1,2] Experimentally, rare-gas atoms are the easiest atomic target particles to obtain, and charge transfer between rare-gas atoms and various ions has been studied several times. Measurements of the charge-transfer cross sections[3–5] are mostly for primary-ion energies above 100 eV, but the light produced by collisions of rare-gas ions and rare-gas atoms has been studied for primary-ion energies as low as 5 eV.[6–9] It is not now clear whether existing theoretical approaches accurately describe the charge-transfer processes occuring in low-energy atomic collisions.[10]

For high primary-ion energies, ion-neutral collisions are known to produce ionization,[5,11,12] but there are only a few studies of ionization produced by low-energy ion-neutral collisions. Moe[13] has measured ionization cross sections for K^+ impinging on the rare gases for primary-ion energies as low as 40 eV, and Rostagni[14] has studied ionization produced by collisions of rare-gas ions and atoms. The cross section for $He^+ + Ar \rightarrow Ar^{++} + He + e$ is fairly large for a primary-ion energy of 100 eV.[15] The theory for these low-energy ionization processes is rather incomplete, perhaps because so few experimental data exist.[1,2,16]

In the present work, collisions between some atomic ions and rare-gas atoms have been investigated. Experimental cross sections are presented for production of Kr^+, Kr^{++}, Xe^+, and Xe^{++} for primary-ion energies between 0.5 and 100 eV. For restricted ranges of primary-ion energies, the secondary ions must be produced by the reactions

$$H^+ + Xe \rightarrow Xe^+ + H, \quad (1)$$

$$H^+ + Kr \rightarrow Kr^+ + H, \quad (2)$$

$$He^+ + Xe \rightarrow Xe^+ + He, \quad (3)$$

$$He^+ + Xe \rightarrow Xe^{++} + He + e, \quad (4)$$

$$He^+ + Kr \rightarrow Kr^+ + He, \quad (5)$$

$$He^+ + Kr \rightarrow Kr^{++} + He + e, \quad (6)$$

$$Ne^+ + Xe \rightarrow Xe^+ + Ne, \quad (7)$$

$$Ne^+ + Xe \rightarrow Xe^{++} + Ne + e, \quad (8)$$

$$Ne^+ + Kr \rightarrow Kr^+ + Ne, \quad (9)$$

$$Ne^+ + Kr \rightarrow Kr^{++} + Ne + e. \quad (10)$$

Several other reactions have also been cursorily examined. Since doubly charged ions are sometimes produced, it appears that free electrons can be produced by low-energy ion-neutral collisions. The experimental data are compared with some of the theoretical results.

II. EXPERIMENTAL PROCEDURE

A schematic diagram of the apparatus is shown in Fig. 1. Detailed descriptions of this apparatus and of the methods used to determine the cross section have been given elsewhere.[17–19] The protons are produced in the ion source by bombarding NH_3 with electrons. The rare-gas ions Ne^+ and

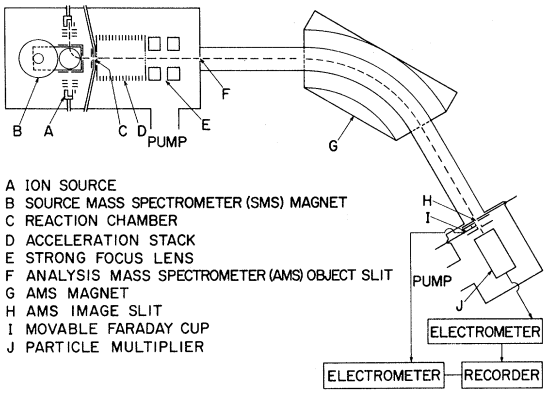

FIG. 1. Schematic diagram of the apparatus (not to scale). Gas is admitted into the ion source through the tube shown, and ions are produced by electron bombardment. The dashed line represents a typical primary-ion trajectory. Regulation and measurement of the target-gas pressure are accomplished through the two tubes connected to the reaction chamber.

He^+ are produced by bombarding Ne and He with electrons having ≈45 and 55–80 eV,[20] respectively. The ions are extracted from the ion source, analyzed in the source mass spectrometer (SMS), and passed into the reaction chamber. The primary- and secondary-ion currents emerging from the reaction chamber are detected by the analysis mass spectrometer (AMS).

The electron energy in the ion source is known to perhaps ±1 eV, and the spread in electron energies is thought to be 1 or 2 eV. Since 48.7 and 65.4 eV are required to excite, respectively, metastable levels of Ne^+ and He^+, excited ions are not expected to be in the primary beam for most of the work reported here.[21]

The data for reaction (5) correspond to He^+ produced by 80 eV electrons. In those cases checked, the cross section for reaction (5) does not seem to depend much on electron energy. Thus, we conclude that the cross sections reported here pertain to reactant ions and atoms in the ground state.

The pressure in the reaction chamber is monitored with a cooled McLeod gauge.[22] The openings in the reaction chamber are large enough that the indicated pressure P_{app}, which is always between 0.8 and 4.2 mTorr, is not the true pressure along the path of the primary ions. Thus, if the target particle density is calculated from P_{app}, then the experimental cross sections must be multiplied by a pressure times length correction factor α. The procedure for determining α has been described elsewhere.[18,23] For the present apparatus, $\alpha = 2.0\,^{+0.2}_{-0.4}$. The cross sections presented in this report have been multiplied by α.[24]

On the average, secondary ions scattered by less than 30° from the direction of the primary-ion beam should emerge from the reaction chamber and be detected, while secondaries scattered at larger angles will, typically, strike the walls of the reaction chamber and be lost. The measured cross sections tend, therefore, to be smaller than the true cross sections. Since the fraction of secondary ions lost may depend on the primary-ion energy, the measured energy dependence may be distorted. This loss of secondary ions depends on the particular reaction studied, and its importance may be hard to assess in any given case.

Define the secondary-ion transmission coefficient K_2 of the reaction chamber by[17]

$$K_2 = \frac{\text{number of ions produced in the reaction chamber}}{\text{number of ions energing from the reaction chamber}} .$$

Previously, with different apparatus, K_2 has been measured for some reactions by electrically accelerating the ions out of the reaction box.[25–27] Applied electric fields may not penetrate into the interior of the reaction chamber used in the present investigations. Thus, the value of K_2 measured by applying a drawout field between the reaction chamber (C in Fig. 1) and the grid between the reaction chamber and the acceleration stack (D in Fig. 1) may be smaller than the true value of K_2; nevertheless, values of K_2 have been estimated by this method, and all of the cross sections presented in the figures are multiplied by the measured values of K_2. It is expected that the measured values of K_2 will be at least one-third of the true values of K_2.[28]

The factor of 3 uncertainty quoted in the previous paragraph is the best quantitative measure of the uncertainty in K_2. This uncertainty is rather large, and a qualitative discussion of the uncertainties in these cross sections may be helpful to future users of these data. The qualitative discussion of uncertainties requires information presented later in the paper, so the details are deferred to Appendix A. Briefly, it is to be expected that the maximum values of the cross sections may be as much as a factor of 2 lower than the true cross sections; however, at least the cross sections for the production of Kr^{++} and Xe^{++} should be even closer to the true cross sections. Major features in the experimental cross sections σ should also be present in the true cross sections.

TABLE I. Energetics and parameters characterizing reactions (1)–(10).

i	Reaction	Q_i [a] (eV)	$E^{\min}_{c.m.}$ [b] (eV)	K [c] (Å^2)	k [c]	δ [c]	$\bar{E}_i$ [d] (eV)	$\lvert\Delta E\rvert_c$ [e] (eV)
(1)	$H^+ + Xe \rightarrow Xe^+ + H$	1.468	12.13	108	0.052	0.0208	12.864	0.0746
(2)	$H^+ + Kr \rightarrow Kr^+ + H$	−0.401	13.999	25	0.030	0.0069	13.799	0.0256
(3)	$He^+ + Xe \rightarrow Xe^+ + He$	12.456	12.13	658	0.055	0.0103	18.358	0.0441
(4)	$He^+ + Xe \rightarrow Xe^{++} + He + e$	−8.744	33.33	•••	•••	•••	•••	•••
(5)	$He^+ + Kr \rightarrow Kr^+ + He$	10.587	13.999	149	0.057	0.0167	19.293	0.0734
(6)	$He^+ + Kr \rightarrow Kr^{++} + He + e$	−13.984	38.57	•••	•••	•••	•••	•••
(7)	$Ne^+ + Xe \rightarrow Xe^+ + Ne$	9.434	12.13	•••	•••	•••	•••	•••
(8)	$Ne^+ + Xe \rightarrow Xe^{++} + Ne + e$	−11.766	33.33	•••	•••	•••	•••	•••
(9)	$Ne^+ + Kr \rightarrow Kr^+ + Ne$	7.565	13.999	8710	0.067	0.058	17.782	0.245
(10)	$Ne^+ + Kr \rightarrow Kr^{++} + Ne + e$	−17.006	38.57	•••	•••	•••	•••	•••

[a] Q_i is the energy released in reaction (i), provided that the reactants and products are unexcited. Ionization potentials E_i are taken from Ref. 44. For endothermic reactions, $Q_i < 0$.

[b] $E^{\min}_{c.m.} = E_i(B)$, where B is the target atom in reactions (1)–(3), (5), (7), and (9). $E^{\min}_{c.m.} = E_i(B) + E_i(B^+)$, where B is the target atom in reactions (4), (6), (8), and (10). For $E_{c.m.} \lesssim E^{\min}_{c.m.}$ the unobserved reaction products must be those indicated in reactions (1)–(10). Ionization potentials are taken from Ref. 44.

[c] Parameters entering into the semiempirical relation (21). The dashed curves in Figs. 2–5 and 7 correspond to these values.

[d] $\bar{E}_i \equiv \frac{1}{2}[E_i(A) + E_i(B)]$ where A^+ is the primary ion and B is the target particle. Ionization potentials are taken from Ref. 44.

[e] $\lvert\Delta E\rvert_c$ is the energy defect for the reaction and is calculated from $\lvert\Delta E\rvert_c = (\bar{E}_i)\,\delta$. See Sec. IV B.

In particular, 20–30% variations in experimental cross sections over wide ranges of primary-ion energies may conceivably be artificial, but variations of factors of 2 or more are probably real.

Except for the secondary-ion collection problem, the measured cross sections are probably within ± 35% of the true cross sections and should represent the relative cross sections as functions of energy to within 15%.[24] When the spread in the primary-ion energy and the uncertainties in determining the mean energy are considered, the kinetic energy of the primary ions should not differ from the quoted mean energy E by more than the larger of $0.02E$ and 0.4 eV. Thermal motion in the target gas may distort some of the measured cross sections.[29]

Finally, only positive ions are detected in this experiment, and the other products in reactions (1)–(10) are inferred. For example, consider the production of Xe^+ in collisions of H^+ and Xe. For $E \leq 12.2$ eV, the Xe^+ secondaries must be produced by reaction (1). When $E \geq 12.2$ eV, the reaction $H^+ + Xe \rightarrow Xe^+ + H^+ + e$ is energetically possible, and it is presently impossible to determine by what process the Xe^+ is produced. Thus, the cross sections in this report are cross sections for the production of a given positive secondary ion.

For certain energy ranges, all of the reaction products are well-defined and are given by reactions (1)–(10). The positively charged secondary ions, say B^+, are observed, so production of B^+ may proceed by either (a) $A^+ + B \rightarrow B^+ + A$ or by (b) $A^+ + B \rightarrow B^+ + A^+ + e$, which is the next energetically possible ionization process; thus B^+ is *known* to be produced by reaction (a) when the kinetic energy $E_{c.m.}$ of the reactants in the center-of-mass (c. m.) system is less than the ionization potential $E_i(B)$ of B. The production of the doubly charged positive ion B^{++} can proceed by either (c) $A^+ + B \rightarrow B^{++} + A + e$, by (d) $A^+ + B \rightarrow B^{++} + A^+ + 2e$, or by (e) $A^+ + B \rightarrow B^{++} + A^-$; the electron affinity of the rare gases should be very small or the negative ion unstable, so production of B^{++} must proceed by reaction (c) for $E_{c.m.} \lesssim E_i(B) + E_i(B^+)$. The unobserved products must be those given in reactions (1)–(10) for $E_{c.m.}$ less than the values $E^{\min}_{c.m.}$ listed in Table I.

III. EXPERIMENTAL RESULTS

Cross sections for reactions (1)–(10) are given in Figs. 2–7. The solid curves in these figures are judged by the author to be sufficiently accurate representations of the data. The dashed curves result from the semiempirical approach that is discussed in Sec. IV B. If the semiempirical curve is judged to represent the data satisfactorily, then no solid curve is given. Error bars are given as indications of probable reproducibility wherever the scatter of the data is not sufficiently indicative. Arrows pointing downward indicate that the cross sections may be zero within experimental error. Scales are given for kinetic energies in the laboratory and c. m. systems.

Several reactions besides (1)–(10) were examined. The reactions

$$H^+ + Xe \rightarrow Xe^{++} + H + e\,, \tag{11}$$

$$H^+ + Kr \rightarrow Kr^{++} + H + e\,, \tag{12}$$

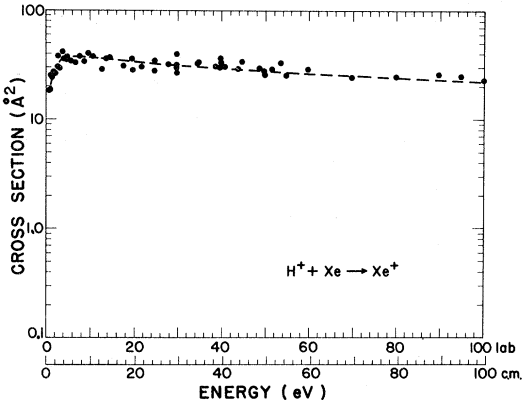

FIG. 2. Cross section for the production of Xe^+ in collisions between H^+ and Xe. Energy scales are given for both the laboratory (lab) and center-of-mass (c.m.) systems. The c.m. scale is the proper one for Xe^{132}. Data are shown as solid circles (•). The dashed curve is the semiempirical curve discussed in Sec. IV B and is judged to be a good representation of the data.

$$H^+ + Ar \rightarrow Ar^{++} + H + e \qquad (13)$$

do not seem to proceed very rapidly when the primary-ion kinetic energy E is less than 100 eV; specifically, the cross sections for these three reactions are less than 2×10^{-4} Å^2 for $E \approx 95$ eV.[30] Since doubly charged target molecules are produced in collisions of Ne^+ with Kr and Xe, it was thought that Ne^{++} might also be produced; however, neither

$$Ne^+ + Xe \rightarrow Ne^{++} + Xe + e \qquad (14)$$

nor

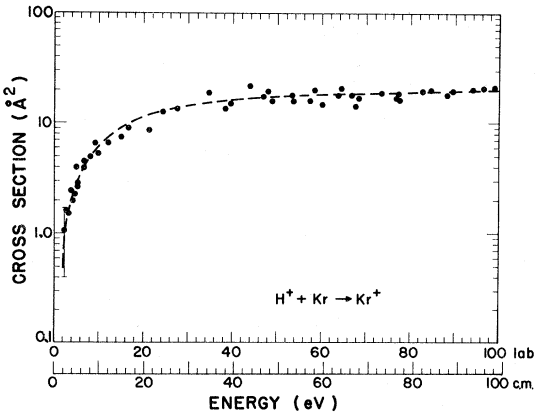

FIG. 3. Cross section for the production of Kr^+ in collisions between H^+ and Kr. The c.m. energy scale is the proper one for Kr^{84}. Data are shown as solid circles (•). The dashed curve is the semiempirical curve discussed in Sec. IV B and is judged to be a satisfactory representation of the data.

$$Ne^+ + Kr \rightarrow Ne^{++} + Kr + e \qquad (15)$$

appears to have significant cross sections when $E \lesssim 100$ eV. Specifically, for $E \approx 54$ eV, the cross section for reaction (14) is less than 5×10^{-3} Å^2. Collisions between He^+ and Ar produce Ar^+ and Ar^{++} with fair-size cross sections for at least several eV below $E = 100$ eV. Collisions between Ne^+ and Ar produce Ar^+ with a fair-sized cross section. Collisions between H^+ and Ar produce Ar^+, but the cross section becomes small as E is decreased below 100 eV.

As can be seen from Table I, all of the pure charge-transfer processes except reaction (2) are exothermic; nevertheless, all of the cross sections for pure charge transfer fall off rapidly at low energies. The maximum values of these cross sections vary from ~0.3 to ~40Å^2. For a given target, a smaller primary-ion mass corresponds to a larger cross section. For a given primary ion, the cross section for producing Xe^+ is larger than the cross section for producing Kr^+, and data not presented here suggest that for the same primary ion the cross section for the production of Ar^+ is still smaller. Thus, it appears that the more complex the target atoms and the lighter the primary ions are, the larger the pure charge trans-

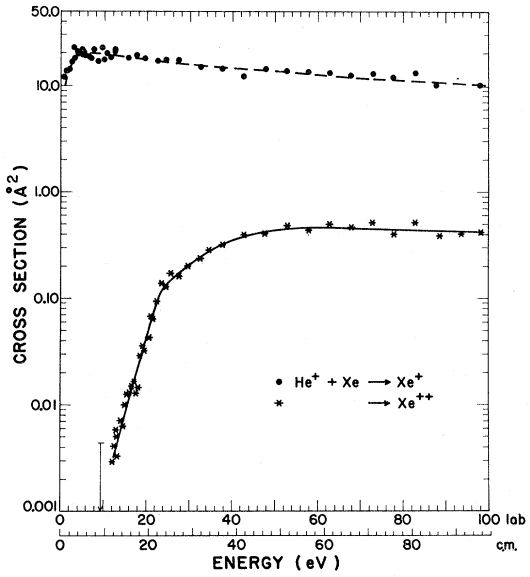

FIG. 4. Cross sections for the production of Xe^+ and Xe^{++} in collisions between He^+ and Xe. The c.m. energy scale is the proper one for Xe^{132}. Solid circles (•) are data for the production of Xe^+, and asterisks (*) are data for the production of Xe^{++}. The arrow indicates the upper limit on the cross section for the production of Xe^{++} when $E \approx 9.5$ eV. The dashed curve is the semiempirical curve discussed in Sec. IV B and is judged to be a good representation of the Xe^+ data. The solid curve satisfactorily represents the Xe^{++} data.

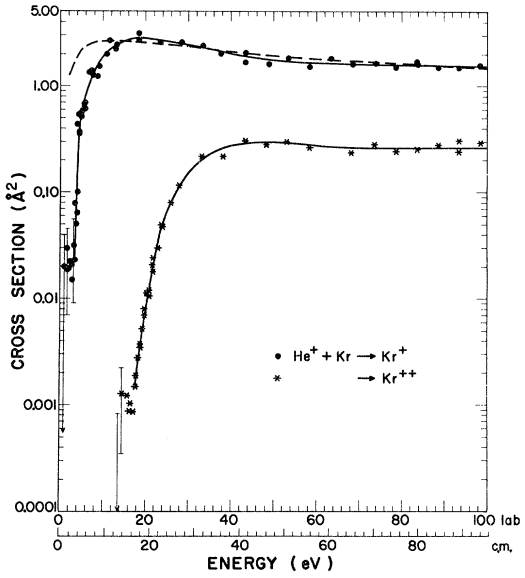

FIG. 5. Cross sections for the production of Kr^+ and Kr^{++} in collisions between He^+ and Kr. The c.m. energy scale is the proper one for Kr^{84}. Solid circles (•) are data for the production of Kr^+ and asterisks (*) are data for the production of Kr^{++}. The error bars are measures of reproducibility. The dashed curve is the semiempirical curve discussed in Sec. IV B, and is a fair representation of the Kr^+ data when and only when the kinetic energy of the primary He^+ is larger than 12 eV. The solid curves are judged to represent the data satisfactorily.

fer-cross sections will be at low collision velocities.

All of the pure charge-transfer cross sections have certain similarities. As E is increased from zero, the cross sections rise rather steeply. The cross section for reaction (2) is nearly constant for $E \gtrsim 40$ eV, but all the other pure charge-transfer cross sections have a maximum value at fairly low energies and then slowly decrease as E is raised. Note that the cross sections for reactions (7) and (9), which involve the most complicated primary ion, Ne^+, fall off more rapidly with increasing E than the other cross sections; this difference in behavior suggests that the mechanisms by which charge transfer proceeds in reactions (7) and (9) may somehow differ from the mechanisms involved in the other four pure charge-transfer reactions.

The cross section for reaction (5) is seen in Fig. 5 to rise very steeply at $E \approx 3$ eV. The true cross section almost certainly rises even faster, because instrumental effects (cf. Sec. II and Ref. 29) cause the slope of the measured cross section to be less than that of the true cross section.

The cross section for reaction (5) appears in Fig. 5 to vary rather slowly for $1 \lesssim E \lesssim 3$ eV; however, the data scatter too much to permit a definite conclusion. The cross section in Fig. 7 for reaction (9) definitely appears to vary rather slowly for $3 \lesssim E \lesssim 8$ eV.

Charge transfer and the simultaneous production of a free electron are observed. Cross sections for this type of process are smaller than the pure charge transfer cross sections. The doubly charged products are first detected 0–4 eV above the true thresholds for the reactions. The cross sections rise rather rapidly to a maximum value as E is increased and then decrease rather slowly. One striking feature of these reactions is that the cross sections reach maxima within 20–40 eV of the threshold energy.

It is noteworthy that the lighter, more rapidly moving, primary ions do not seem to produce free electrons more efficaciously than the heavier primary ions. In particular, no doubly charged secondary ions were observed in collisions of H^+ with Kr and Xe.[31] This behavior differs from that for pure charge transfer, where cross sections are larger for reactions involving lighter primary ions.

In low-energy ion-neutral collisions the production of doubly charged positive ions is sometimes fairly probable and sometimes not. Further investigation will be required before this interesting but little-studied phenomenon is understood.

IV. DISCUSSION

A. Comparison with Previous Experimental Work

Koopman[3] has measured total "charge-exchange

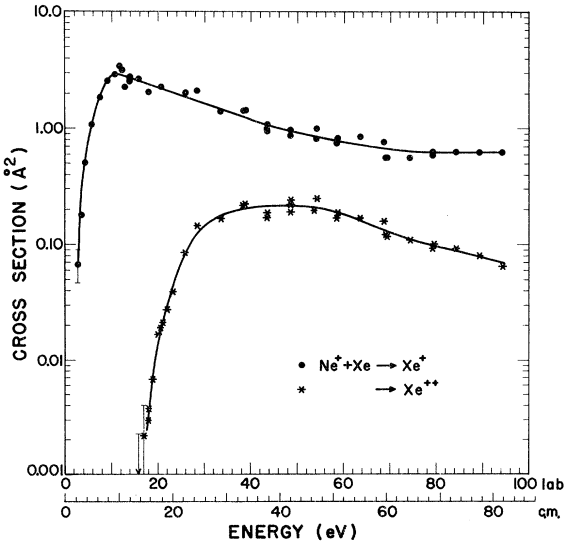

FIG. 6. Cross sections for the production of Xe^+ and Xe^{++} in collisions between Ne^+ and Xe. The c.m. energy scale is the proper one for Xe^{132}. Solid circles (•) are data for the production of Xe^+ and asterisks (*) are the data for the production of Xe^{++}. The error bars are measures of reproducibility. The solid curves are judged to represent the data satisfactorily.

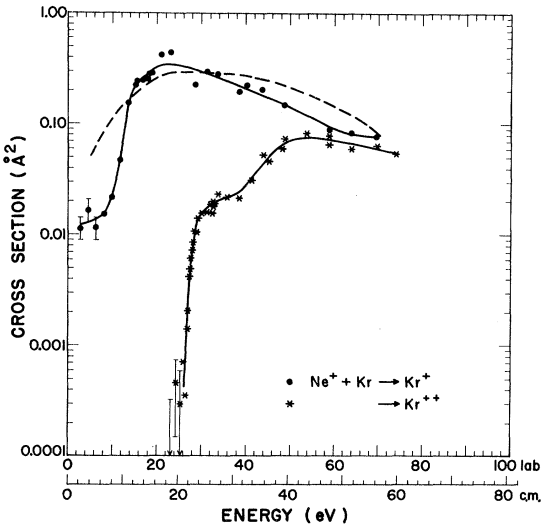

FIG. 7. Cross sections for the production of Kr^+ and Kr^{++} in collisions between Ne^+ and Kr. The c.m. energy scale is the proper one for Xe^{132}. Solid circles (•) are data for the production of Kr^+ and asterisks (*) are data for the production of Kr^{++}. The dashed curve is the semi-empirical result discussed in Sec. IVB and does not represent the data satisfactorily. The solid curves are satisfactory representations of the data.

cross sections" of reactions (1)–(3) and (5) for primary-ion energies above 70 eV. His cross sections are compared with the present results in Table II. Although Koopman's cross sections are as much as a factor of 2 higher than the present results, the dependences of his cross sections on E agree, within the experimental errors, with the results of this investigation. It has been noted in Sec. II that the present cross sections may be as much as a factor of 3 lower than the true cross sections. Thus, there are no irreconcilable differences between these results and Koopman's.

While Koopman's[3] cross sections for reactions (1)–(3) and (5) may be nearer to the true magnitudes at $E \approx 70$–100 eV than are the present cross sections, this author believes that Koopman's[3] cross section for charge transfer in $H^+ + H_2$ is too high.[19] Since Koopman measured all of his cross sections on the same apparatus, it is difficult to know just what significance to attach to these differences. In any event, Koopman's results agree fairly well with the present data.

Stedeford and Hasted[4] have measured charge-transfer cross sections for E as low as 100 eV, but their energy range does not extend much below 200 eV for any of the reactions examined in this work. Nevertheless, their cross sections at low ion energies appear to fall too rapidly to be consistent with either the energy dependences or the magnitudes of the present cross sections.

Cross sections for the production of light by ion impact on rare gases have been measured to fairly low primary-ion kinetic energies. Specifically, collisions of He^+ and Ne^+ with Kr and Xe have been studied, and some or all of the light produced is emission from Kr^+ and Xe^+.[6,9] If the light produced in these collisions is Kr II and Xe II emission, then the cross sections for the production of this light must be no larger than the cross sections for the production of Kr^+ and Xe^+. The cross sections measured by Lipeles *et al.*[6] for light with wavelengths $\lambda < 3500$ Å show considerable structure, but the more detailed cross sections of Schlumbohm[9] for light with $\lambda > 3500$Å are almost constant except at low energies, where the cross sections fall to zero.

The cross sections of Lipeles *et al.*[6] for the production of light with wavelengths between 200 and 3500 Å are given in Table III. The present

TABLE II. Experimental cross sections (in Å²) for the production of singly charged secondary ions in various collisions. The upper values are the present data; the lower values are Koopman's (Ref. 3) cross sections.

Reaction[a]	E[b] 70 eV	100 eV
(1) $H^+ + Xe \rightarrow Xe^+ + H$	25	22
	40	40
(2) $H^+ + Kr \rightarrow Kr^+ + H$	18.5	20
	17.4	20
(3) $He^+ + Xe \rightarrow Xe^+ + He$	12	10.5
	14.5	15
(5) $He^+ + Kr \rightarrow Kr^+ + He$	1.6	1.5
		2.4

[a]The present values are actually cross sections for the production of Kr^+ and Xe^+.

[b]$E \equiv$ laboratory kinetic energy of the primary ions.

TABLE III. Comparison of experimental cross sections for the production of light and for the production of Kr^+ and Xe^+ in collisions of He^+ with Kr and Xe. Cross sections are in Å². The upper values are the present cross sections; the lower values are cross sections for the production of light. (The cross sections for the production of light are taken from Lipeles *et al.*, Ref. 6, and include light emitted between 200 and 3500 Å. See Sec. IV A.)

E[a] (eV)	(3) $He^+ + Xe \rightarrow Xe^+ + He \rightarrow$ light	(5) $He^+ + Kr \rightarrow Kr^+ + He \rightarrow$ light
100	10.5	1.5
	5.7	2.6
50	13.7	1.8
	5.5	2.3
20	17.6	2.8
	5.4	2.8
10	20.0	1.9
	9.3	1.2

[a]$E \equiv$ laboratory kinetic energy of the primary ion.

cross sections for reactions (3) and (5) are given for comparison. Because the pertinent spectral information is not given by Lipeles *et al.*, some of the light detected by them may be emission from species other than Kr II and Xe II. Their cross section for the light produced by $He^+ + Xe$ is smaller than the present cross section for reaction (3). Their cross section for light produced by $He^+ + Kr$ is comparable to the present cross section for reaction (5).

Schlumbohm[9] has measured cross sections for the production of visible light in rare-gas-ion–atom collisions, but he does not give total cross sections for the production of visible light except at $E = 200$ eV. His cross sections at $E = 200$ eV for Kr II emission produced by collisions of He^+ and Ne^+ with Kr are 0.92 and 0.71 Å^2, respectively, but are probably low by a factor of 2–2.5.[9,22] The present cross sections for reactions (5) and (9) at $E = 100$ and 70 eV, respectively, are 1.5 and 0.079 Å^2 and are thus smaller than Schlumbohm's corrected cross sections. If Schlumbohm's cross sections are correct, then the cross sections for producing Kr^+ must rise considerably between $E \approx 70$ and 200 eV.

Comparisons of the charge-transfer cross sections with the cross sections for the production of light suggest that a rather large fraction of the singly charged secondary ions are excited.

Fair-sized cross sections for the production of free electrons in ion-neutral collisions have been found by Gilbody and Hasted[12] for primary-ion energies E as low as 25 eV. The emphasis in their measurements is on rather high primary-ion energies, so details of the cross sections for $E \leq 100$ eV are not given in their paper. Furthermore, they did not measure any cross section measured in this work. Their ionization cross sections and the present cross sections for the production of doubly charged secondary ions are about the same order of magnitude.

Moe[13] has measured cross sections for the ionization of the rare gases by K^+. His cross sections are thus not directly related to the present results, but one may still make some interesting comparisons. (a) His cross sections for the production of free electrons are the same order of magnitude as the present cross sections for production of doubly charged ions. (b) His cross sections rise monotonically and slowly between their apparent threshold energies and 250 eV. (c) His apparent threshold energies are further from the true threshold energies than found here. (d) His cross sections seem to have several small "steps" of the sort seen in Fig. 7 of this paper. The differences between Moe's and the present results may well be because different reactions were studied.

Finally there are not many comparable investigations of pure charge transfer or of concomitant charge transfer and ionization in low-energy collisions of atomic ions and atoms. The present data agree fairly well with the results of previous investigations.

B. Comparison with Theory

Rapp and Francis[32] have formulated an approximate theory of asymmetric charge transfer. Their approach has been slightly modified by Lee and Hasted,[33] who give

$$\sigma = f\sigma_0 I(u_1) \tag{16}$$

for the asymmetric charge-transfer cross section σ, where f is a statistical weighting factor. σ_0 is the cross section appropriate for symmetric resonant charge transfer,

$$\sigma_0^{1/2} = k_1 - k_2 \ln v , \tag{17}$$

where k_1 and k_2 are constants and v is the initial speed of the primary ion. $I(u_1)$ is tabulated by Lee and Hasted[33] and

$$I(u_1) = 4 \int_0^{u_1} u^3 \operatorname{sech}^2 u \, du . \tag{18}$$

Formulas relating u_1 and v are also given by Lee and Hasted.

Rapp and Francis[32] point out that their approximations are invalid unless

$$\gamma\rho/a_0 \gg 1, \tag{19}$$

where ρ is the impact parameter, a_0 is the Bohr radius, and

$$\gamma = (E_i/13.6)^{1/2} . \tag{20}$$

E_i is some appropriate ionization potential. If the cross section is fairly large, e.g., much greater than $\pi(a_0/\gamma)^2$, then regions where ρ is not much greater than a_0/γ do not contribute much to the cross section, and Eq. (16) should be valid. For the pure charge-transfer reactions herein, $\gamma \sim 1$, and Eq. (16) can be expected to represent accurately only those cross sections that are considerably larger than 1 Å^2.

As $v \to 0$, Eq. (16) yields $\sigma \to Cv^4$, where C is a constant. Rapp and Francis[32] point out that the result $\sigma \to Cv^4$ is very sensitive to one of their assumptions and that, even for small v, it should not seriously be expected that $\sigma \propto v^4$ will be a good approximation.

The parameters E_i, ΔE, and $\bar{\rho}_1$ enter into the Rapp and Francis theory,[32,33] where ΔE is the "energy defect" and $\bar{\rho}_1$ is a certain impact parameter.[34] The values for these three parameters are not *a priori* known. In addition, our experimental cross sections may be lower than the true cross sections. For these reasons, a semi-

empirical approach is adopted in the comparison of these experimental results with Eq. (16).

Suppose that

$$\sigma = K(1 - k\ln v)^2 I(u_1), \tag{21}$$

where K and k are constants and $I(u_1)$ is tabulated.[33] We have

$$u_1 = \delta G \tag{22}$$

with

$$\delta = |\Delta E| / E_i^{1/2}, \tag{23}$$

where G is a function tabulated by Lee and Hasted.[33] K, k, and δ are then chosen so that Eq. (21) provides a good representation of the experimental data.[35] Cross sections computed from the semiempirical relation [Eq. (21)] are plotted in Figs. 2–5 and 7 for the values of the parameters K, k, and δ given in Table I.

Equation (21) satisfactorily represents the cross sections for reactions (1)–(3). These experimental cross sections are considerably larger than 1 Å^2 over most of the energy range. The drop in experimental cross section at low energies, as E is decreased, is very well reproduced.

Equation (21) is judged to be only a fair representation of the cross section for reaction (5) when $E \gtrsim 12$ eV. The cross section for reaction (5) is about 2 Å for $E \gtrsim 12$ eV. The falloff of the cross section at low energies, as E is decreased, is not even approximately reproduced.

Most of the other cross sections reported here are less than 1 Å^2. Equation (21) does not satisfactorily represent any of these cross sections.[35] In Fig. 7 the semiempirical curve is judged not to represent satisfactorily the cross section for $Ne^+ + Kr \rightarrow Kr^+ + Ne$; a three-parameter "fit" to the experimental data must represent the data very well or be rejected. It is also impossible to represent the data for $Ne^+ + Xe \rightarrow Xe^+ + Ne$ satisfactorily; a semiempirical curve computed from Eq. (21) is, therefore, not given.

The parameter K in Eq. (21) has no particular significance, partly because the experimental cross sections for the pure charge transfer reactions may be lower than the true cross sections.

δ in Eq. (22) is related by Eq. (23) to the energy separation or "defect" $|\Delta E|$ between the potential energy curves of the A^+B state and the B^+A state at the point where $A^+B \rightarrow B^+A$.[36] The proper value of E_i is unknown, but Lee and Hasted[33] suggest setting $E_i = \bar{E}_i$, the mean of the ionization potentials of the two colliding reactants. Then we may calculate values of $|\Delta E|$ from

$$|\Delta E|_c = (\bar{E}_i)^{1/2}\,\delta\,. \tag{24}$$

Values of $|\Delta E|_c$ are given in Table I and range from about 0.025 to 0.25 eV.[37]

k can be estimated from a formula given by Rapp and Francis.[32] k depends on $\bar{\rho}_1$ and E_i, which are not known with precision; however, reasonable choices for $\bar{\rho}_1$ and E_i give $0.03 \lesssim k \lesssim 0.06$. From Table I it can be seen that k is indeed within these limits, except for reaction (9), where Eq. (21) does not represent the data very well.

Some sets of the parameters K, k, and δ other than the sets given in Table I may produce semiempirical curves that will adequately represent the data. For example, the curve that is drawn in Fig. 3 is practically indistinguishable from the curve obtained from Eq. (21) with $K = 11.8$, $k = 0$, and $\delta = 0.0146$.

These results can be summarized as follows. If a charge-exchange cross section is fairly large, then the relations given by Lee and Hasted[33] are expected to represent the data satisfactorily, and they do. Small charge-exchange cross sections are not satisfactorily represented by the formulas given by Lee and Hasted.

It is possible that reactions of the type $A^+ + B \rightarrow B^{++} + A + e$ may proceed in two steps, viz., first $A^+ + B \rightarrow B^{+*} + A$ and then $B^{+*} \rightarrow B^{++} + e$. If so, then the Rapp and Francis[32] theory of charge transfer might describe the reactions producing doubly charged secondaries. In fact, however, the cross sections for these reactions are small and thus the formulas given by Lee and Hasted[33] cannot be expected to,[32] and do not, represent the data adequately.

Since Eq. (21) accurately represents only a few of the reaction cross sections, it is necessary to consider what other theoretical approaches may satisfactorily describe the other reactions.

Schlumbohm[9] gives a very simple formula

$$\sigma = C_1[1 - (E_{th}/E_{c.m.})] \tag{25}$$

that he says represents his data within 20%, where $E_{c.m.} \equiv$ c. m. kinetic energy of the reactants, C_1 is a constant, and E_{th} is the threshold energy of the reaction. If E_{th} is taken to be the apparent threshold energy, then Eq. (25) represents some of the cross sections within 40%, but, in general, the agreement with the data is not impressive. Of course, if there were several thresholds, then the cross sections would be a sum of terms like Eq. (25), but the possibility of representing the data by such a formula is not further explored here.

Since three particles are produced in $A^+ + B \rightarrow B^{++} + A + e$, the formula

$$\sigma = K(E_{c.m.} - E_{th})^2 / E_{c.m.}^{1/2}. \tag{26}$$

might accurately represent the rising portions of those cross sections.[38,39] If the apparent threshold energies are used for E_{th}, then Eq. (26) is a fair representation of the rising part of the mea-

sured cross sections. None of these curves are shown, because there are no strong reasons for supposing that Eq. (26) will accurately represent the cross sections for $A^+ + B \rightarrow B^{++} + A + e$.

Neither Eq. (25) nor Eq. (26) is really likely to provide an adequate representation of the reactions studied in this work, because the theory behind these equations is too simple to be realistic.

Mott and Massey[1] give formulas for charge transfer which differ from the formulas of Rapp and Francis.[32] Basically, the formulation given by Mott and Massey is a Landau-Zener treatment of charge transfer occurring at a crossing point[40] of the potential energy curves of the A^+B and B^+A states.[36] The formulas in Mott and Massey may be put in the form (see Appendix B)

$$\sigma = A(E-\epsilon)\, J(\xi)/E, \tag{27}$$

where

$$\xi^{-2} = \beta(E-\epsilon), \tag{28}$$

and E is the primary-ion energy; A, β, and ϵ are constants; and $J(\xi)$ is given by Moiseiwitsch.[41] As $\xi^{-2} \rightarrow 0$, $J(\xi)$ drops rapidly to zero, and as $E \rightarrow \epsilon$, σ in Eq. (27) goes to zero. Thus ϵ can be regarded as the apparent threshold energy for a reaction that is suitably described by Eq. (27). Taking a semiempirical approach and choosing A, β, and ϵ such that the best representations of the data by Eq. (27) are obtained,[35] one finds that Eq. (27) does not satisfactorily fit the cross sections reported in this paper, although the portions of the cross sections that rise as E is increased can be reproduced fairly well in some cases.

C. Further Discussion

Most of the cross sections reported here are not reproduced by any of the theoretical formulas examined. Expressions[33] having the form found by Rapp and Francis[32] represent well the larger, experimental charge-transfer cross sections; this impressive agreement may be fortuitous, but the Rapp and Francis theory seems to fit only the data that it is expected to fit.

Formulation of the problem in terms of charge transfer at a single crossing of potential curves yields formulas that do not represent the experimental data very well. On the other hand, potential energy curves for a given diatomic ion may have many crossings,[40] and the cross section for pure charge transfer or charge transfer with associated ionization should be some appropriate sum over contributions from all of the crossing points.[42,43] It is not, therefore, too surprising that Eqs. (27) and (28) do not accurately represent the experimental data.

All of the cross sections presented here have one or more rather sharp increases as E is increased. Some of these increases are consistent with the predictions of the Rapp and Francis theory, but those associated with the smaller cross sections cannot be understood in this way. The onset energies of these increases in the cross sections may suggest some explanation for the phenomena.

Consider the cross section in Fig. 7 for the production of Kr^+. As $E_{c.m.}$ decreases below 18 eV, the cross section drops until $E_{c.m.} = 6.2 \pm 0.8$ eV, below which energy the measured cross section appears to level off. Write, for reaction (9),

$$Q_{app} = -6.2 \text{ eV} = E_i(\text{Ne}) - E_i(\text{Kr}) - \mathcal{E}(\text{Kr}^{+*}), \tag{29}$$

where $-Q_{app}$ is the apparent threshold energy in the c.m. system and $\mathcal{E}(Kr^{+*})$ is the energy with which Kr^{+*} is assumed to be excited. One finds[44]

$$\mathcal{E}(\text{Kr}^{+*}) = 13.77 \pm 0.8 \text{ eV}. \tag{30}$$

Likewise, although reaction (5) is exothermic, the corresponding cross section in Fig. 5 has an apparent threshold, and

$$Q_{app} = -2.9 \pm 1 \text{ eV} = E_i(\text{He}) - E_i(\text{Kr}) - \mathcal{E}(\text{Kr}^{+*}), \tag{31}$$

$$\mathcal{E}(\text{Kr}^{+*}) = 13.49 \pm 1 \text{ eV}. \tag{32}$$

These two values of $\mathcal{E}$ are within experimental accuracy of each other and are fairly close to the energy, 13.514 eV, of Kr^+ ($^2S_{1/2}$) above the ground state of Kr^+.[45]

The author knows of no reason for Kr^+ ($^2S_{1/2}$) to be preferentially excited in reactions (5) and (9), and it may be that the separating reaction products possess $\approx$13.5 eV of kinetic energy. On the other hand, there are no states of Kr^+ between the $^2P^0$ (ground state) multiplet levels and the $^2S_{1/2}$ level, and there are several Kr^+ states just above the $^2S_{1/2}$ state. Thus, the number of energetically available Kr^+ states increases rather rapidly above 13.5 eV,[45] i.e., as $E_{c.m.}$ is increased above 6.2 eV for reaction (9) and 2.9 eV for reaction (5). Perhaps, the increases in the cross sections for reactions (5) and (9) are ascribable to this increase in the number of available excited states of Kr^+.

Some of the other increases in cross sections can be roughly correlated with the number of available excited states of the reaction products. In Fig. 7, there are two sudden increases in the cross section for the production of Kr^{++}, at $Q_{app} = -21 \pm 2$ eV and $Q_{app} = -31 \pm 2$ eV. These values of Q_{app} yield

$$\mathcal{E}(\text{Kr}^{++*}) = 4 \pm 2 \text{ eV}, \tag{33}$$

$$\mathcal{E}(\text{Kr}^{++*}) = 14 \pm 2 \text{ eV}. \tag{34}$$

There are states of Kr^{++} at 1.816, 4.101, and

14.373 eV, and the density of Kr^{++} excited states is greater for energies above 14.37 eV than for energies below 14.37 eV.[45] Similarly, the onset energy for reaction (7) is estimated to be 1.8 ±1.5 eV corresponding to

$$\mathcal{E}(Xe^{+*}) = 11.23 \pm 1.5 \text{ eV}.$$

Xe^+ ($^2S_{1/2}$) is 11.266 eV above the ground state of Xe^+, and the density of Xe^+ excited states is considerably greater above than below 11.26 eV. The data for reactions (4), (6), and (8) are not inconsistent with the notion that increases in cross sections are associated with excited product states becoming energetically available.

It is thus possible to correlate the energies at which increases occur in the smaller cross section with increases in the number of available states of the reaction products. The present data are not precise enough to be really convincing about this point, and more work is needed.

V. CONCLUSIONS

The major findings of this investigation may be summarized as follows.

(a) Low-energy ion-neutral collisions appear to produce free electrons. Specifically, reactions like $A^+ + B \rightarrow B^{++} + A + e$, involving concomitant charge transfer and ionization, appear to have fair-sized cross sections whenever the reaction is energetically possible. It is possible that ionization may occur in many other ion-neutral collisions. Apparent threshold energies for electron production are 0–4 eV above the minimum energies required.

(b) The pure charge-transfer cross sections measured here are, for a given primary ion, larger when the target atom has more electrons.

(c) The pure charge-transfer cross sections measured here are, for a given target atom, larger when the primary ion is less massive.

(d) These experimental cross sections are consistent with previous experimental data.

(e) The semiempirical formula taken from relations in Lee and Hasted[33] is a good representation of the larger pure charge-transfer cross sections but is not a good representation of the smaller pure charge-transfer cross sections. These findings are the theoretically expected results.[32]

(f) Increases in the smaller cross sections as E is increased can be roughly correlated with the energies of excited states of the reaction products. It appears that the accessibility of new reaction channels leading to different states of the reaction products may be responsible for the increases in the smaller cross sections.

(g) The experimental results for the production of doubly charged positive ions and free electrons are not well understood. More experimental and theoretical study of these ionization reactions is needed.

ACKNOWLEDGMENTS

The author wishes to thank H. W. Hoerlin, D. M. Kerr, and H. M. Peek for the support given this project. I am grateful to Bruce Stewart, who collected most of the data presented herein, and to many other members of Group J-10 of the Los Alamos Scientific Laboratory for their assistance. I am grateful to R. F. Holland and M. S. Tierney for their valuable advice.

APPENDIX A: FURTHER DISCUSSION OF EXPERIMENTAL UNCERTAINTIES

A detailed qualitative discussion of the uncertainties in these results due to uncertainties in K_2 depends on three things: (a) calculated estimates of the number of secondary ions lost to the reaction chamber walls, (b) values of K_2 measured by applying a potential to the reaction chamber (see Sec. II), and (c) previous experiences.

First, consider the calculations. Define $v_c \equiv$ velocity of the c.m. of the colliding reactants, $v_b' \equiv$ velocity of the secondary ion in the c.m. system, $\gamma \equiv v_c/v_b'$. The angular distributions of secondary ions in the laboratory depend on γ and on the angular distributions of secondary ions in the c.m. system.

Some of the reactions studied here are endothermic, and for these reactions, $\gamma \geq 1$. Secondary ions produced in these reactions would be scattered by less than 90° from the primary-ion beam direction in the laboratory, if the target molecules were stationary. Secondary ions scattered by less than 30° should be detected, and more than 35% of the secondary ions produced in reactions where $\gamma \geq 1$ may be scattered by less than 30°.[46,47] Near the threshold energy of an endothermic process, γ is large, and the secondary ions have nearly the same direction in the laboratory as the primary ion. Thus, for the endothermic reactions, one expects that the cross sections are accurate near the threshold energy and not more than a factor of 3 lower than the true cross sections at higher energies, even if it is presumed that $K_2 = 1$. Since the measured cross sections have been multiplied by values of K_2 which are > 1, probably the measured cross sections are within a factor of 2 of the true cross sections.

The values of $|\Delta E|$ in Table I and the discussion in Sec. IV C suggest that those reactions which can proceed through reaction channels that release large amounts of energy may nevertheless proceed through channels which are endothermic or which release small amounts of energy. In such case, $\gamma \gtrsim 1$, and the comments in the preceding paragraph apply.

The results in Ref. 38 suggest that fairly drastic changes in angular distributions of secondary ions

in the c.m. system would be required to produce large effects in cross sections measured with the present apparatus as E is changed.

Now consider the values of K_2 measured by applying a potential to draw the secondary ions out of the reaction chamber. For a variety of reasons it is expected that when a rather small value of K_2 is measured for a reaction then the resulting cross section is fairly accurate. This hypothesis has been borne out in those cases where an accurate check has been made[28]; however, there are not enough such checks. Rather small (≤ 1.3) values of K_2 are measured for reactions (8) and (10), and moderate values (< 2.7) of K_2 are measured for the other reactions.[48] These values of K_2 suggest that most of the secondary ions are collected when the ions are drawn out of the reaction chamber and that the cross sections presented in this report are within a factor of 2 of the true cross sections at fairly high primary-ion kinetic energies.

Previous experience has yielded three items of information pertinent to the present discussion.

The reaction chamber used in the present investigation is not so open as another reaction chamber that is sometimes used. Cross sections measured with these two chambers occasionally differ somewhat in magnitude, but the qualitative aspects of the cross sections are similar.[49] Since there are no important differences in the qualitative appearances of cross sections measured with different apertures for collection of secondary ions, we suppose that the qualitative behavior of the measured cross sections is similar to that of the true cross sections.

All of the present cross sections decrease rather rapidly as E is lowered below some energy. The decreases are, in the author's opinion, probably real; however, the falloff is probably more rapid than these data indicate because of the thermal energy of the target atoms and the spread in primary-ion energies.

Some of the cross sections previously measured with this apparatus are in very good agreement with cross sections measured elsewhere.[24,25,50] Such agreement gives some confidence that the data taken with this apparatus are properly treated and understood. Unfortunately, there are also cases where measurements made with this apparatus disagree with other measurements.

The inferences drawn from these discussions are summarized in Sec. II. The opinions expressed in this appendix should be helpful in assessing the data; however, the qualitative nature of these remarks should be kept in mind.

APPENDIX B

Mott and Massey[51] give the cross section for charge transfer due to a potential curve crossing[40] as

$$\sigma \approx (4\pi/k_0^2)\, f \int_0^L (l+\tfrac{1}{2})\, e^{-2\gamma_l}\,(1-e^{-2\gamma_l})\, dl, \tag{B1}$$

where f is a statistical weight factor,[51] L is the quantum number of the maximum orbital angular momentum for which there are contributions to σ, $k_0 = \mu v/\hbar$, $\mu \equiv$ reduced mass of the reactants, and v is the speed with which the reactants initially approach each other. We have

$$\gamma_l = b/v_l\,, \tag{B2}$$

$$v_l = (\hbar/\mu)\,[k_0^2 - U_{00}(R) - (l+\tfrac{1}{2})^2/R^2]^{1/2}\,, \tag{B3}$$

where l is the quantum number for the orbital angular momentum of the colliding reactants and R is the internuclear separation at which the crossing point of the potential curves occurs. Here, U_{00} and b are treated as unknown constants. Set

$$\gamma_l = \tfrac{1}{2}\eta\, x\,, \tag{B4}$$

with

$$x = [\,1 - U_{00}/k_0^2 - (l+\tfrac{1}{2})^2/(k_0 R)^2]^{-1/2} \tag{B5}$$

and with

$$\eta = \mu b/\hbar k_0 = b/v\,. \tag{B6}$$

Then Eq. (B1) is approximately[52]

$$\sigma \approx 4\pi f\, R^2 \int_{x_0}^{\infty} x^{-3}\, e^{-\eta x}\,(1-e^{-\eta x})\, dx\,, \tag{B7}$$

with

$$x_0 = (1 - U_{00}/k_0^2)^{-1/2}\,. \tag{B8}$$

Let

$$\xi = x/x_0\,. \tag{B9}$$

Then we have

$$\sigma \approx 4\pi f\, R^2 x_0^{-2} \int_1^{\infty} \xi^{-3}\, e^{-\eta x_0 \xi}\,(1-e^{-\eta x_0 \xi})\, d\xi \tag{B10}$$

or

$$\sigma \approx 4\pi f R^2\,(1 - U_{00}/k_0^2)\, J(\eta x_0)\,. \tag{B11}$$

The function J is given by Moiseiwitsch.[41] Now, one can write

$$(\eta x_0)^{-2} = v^2\,(1 - U_{00}/k_0^2)/b^2 \equiv \beta(E-\epsilon)\,, \tag{B12}$$

where β and ϵ are constants.

In this paper, a semiempirical approach is adopted, and we write

$$\sigma = A(E-\epsilon)\, J(\xi)/E\,, \tag{B13}$$

where

$$\xi^{-2} \equiv \beta(E-\epsilon)\,. \tag{B14}$$

A, β, and ϵ are arbitrary constants, and $J(\xi)$ is given by Moiseiwitsch.[41]

*Work conducted under the auspices of the United States Atomic Energy Commission.

[1]N. F. Mott and H. S. W. Massey, *The Theory of Atomic Collisions*, 3rd ed. (Oxford U.P., London, 1965).

[2]J. B. Hasted, *Physics of Atomic Collisions* (Butterworths, London, 1964).

[3]D. W. Koopman, Phys. Rev. 154, 79 (1967).

[4]J. B. H. Stedeford and J. B. Hasted, Proc. Roy. Soc. (London) A227, 466 (1955).

[5]H. B. Gilbody, J. B. Hasted, J. V. Ireland, A. R. Lee, E. W. Thomas, and A. S. Whitman, Proc. Roy. Soc. (London) A274, 40 (1963).

[6]M. Lipeles, R. Novick, and N. Tolk, Phys. Rev. Letters 15, 815 (1965).

[7]N. H. Tolk, C. W. White, S. H. Dworetsky, and L. A. Farrow, Phys. Rev. Letters 25, 1251 (1970).

[8]D. Jaecks, F. J. De Heer, and A. Salop, Physica 36, 606 (1967).

[9]H. Schlumbohm, Z. Naturforsch. 23a, 970 (1968) [English transl. AFCRL Report No. AFCRL-69-0236, 1969 (unpublished)]. Schlumbohm's cross sections are based on the cross sections of D. T. Stewart [Proc. Phys. Soc. (London) 69, 437 (1956)] and are thus probably low. See Ref. 22.

[10]Compare, for example, the statements in Refs. 6 and 15 with the results in Refs. 2 and 16.

[11]Other references can be found in Refs. 1, 2, and 16.

[12]H. B. Gilbody and J. B. Hasted, Proc. Roy. Soc. (London) 240, 382 (1957).

[13]D. E. Moe, Phys. Rev. 104, 694 (1956).

[14]A. Rostagni, Nuovo Cimento 11, 99 (1934).

[15]R. L. Champton and L. D. Doverspike, in *Sixth International Conference on the Physics of Electronic and Atomic Collisions, Abstracts of Papers* (MIT Press, Cambridge, Mass., 1969), p. 312.

[16]J. B. Hasted, in *Advances in Atomic and Molecular Physics*, edited by D. R. Bates and I. Estermann (Academic, New York, 1968), Vol. 4, p. 237.

[17]C. F. Giese and W. B. Maier II, J. Chem. Phys. 39, 739 (1963).

[18]W. B. Maier II, J. Chem. Phys. 42, 1790 (1965).

[19]W. B. Maier II, J. Chem. Phys. 54, 2732 (1971).

[20]Most of the He^+ used in this study was produced by 55-eV electrons; however, the data for reaction (5) correspond to He^+ primaries produced by 80-eV electrons impinging on He.

[21]C. E. Moore [Natl. Bur. Std. Circ. No. 467 (U. S. GPO, Washington, D. C., 1949), Vol. I] places the $^2S_{1/2}$ state of He^+ at 40.809 eV above the ground state of He^+. The lowest, long-lived state of Ne^+ is 0.097 eV above the ground state, but even if excited, this state will not be distinguishable from the ground state in this work. The $^4P_{5/2}$ state of Ne^+ is 27.167 eV above the ground state of Ne^+.

[22]R. F. Holland, Los Alamos Scientific Laboratory Report No. LA-3783, 1967 (unpublished).

[23]α is called the "pressure-length correction factor" in Ref. 18.

[24]W. B. Maier II and E. Murad [J. Chem. Phys. 55, 2307 (1971)] have compared their cross sections for $N^+ + N_2 \rightarrow N_2^+ + N$. Murad's reaction chamber was similar to the reaction chamber used here; however, Murad did not feel justified in multiplying his cross section by a pressure times length correction factor. Murad's cross section for $N^+ + N_2 \rightarrow N_2^+ + N$ is a factor of 1.7 smaller than Maier's; thus, there is a possibility that the present results are roughly a factor of 2 higher than the true cross sections. See Ref. 18 for further discussion.

[25]W. B. Maier II, Planetary Space Sci. 16, 477 (1968).

[26]W. B. Maier II, J. Chem. Phys. 47, 859 (1967).

[27]W. B. Maier II, J. Chem. Phys. 55, 2699 (1971).

[28]Reactions of the type $A^{++} + B \rightarrow B^+ + A^+$ have been used to estimate the errors in the K_2 values measured by applying drawout fields to the reaction chamber, W. B. Maier II (unpublished).

[29]P. J. Chantry, J. Chem. Phys. 55, 2746 (1971).

[30]More precisely, as noted in the last two paragraphs of Sec. II, the cross section for the production of these doubly charged rare-gas ions in collisions between H^+ and the rare-gas atoms is less than 2×10^{-4} Å^2.

[31]Of course, above the $E_{c.m.}^{min}$ given in Table I, reactions of the type $A^+ + B \rightarrow B^+ + A^+ + e$ may occur. Whether such reactions are important in low-energy, ion-neutral collisions is presently unknown.

[32]D. Rapp and W. E. Francis, J. Chem. Phys. 37, 2631 (1962).

[33]A. R. Lee and J. B. Hasted, Proc. Phys. Soc. (London) 85, 673 (1965).

[34]$\overline{\rho}_1$ is called $\overline{b}_1$ by Rapp and Francis, Ref. 32. They show that k_1 depends on $\overline{\rho}_1$.

[35]Several sets of parameters were tried, and the set that seemed to provide the best representation of the data was chosen. A more formal mathematical procedure, such as a least-squares fit, was not attempted.

[36]The symbol A^+B here simply denotes a molecular ionic state for which the potential energy curve corresponds to A^+ and B at infinite internuclear separations.

[37]Lipeles *et al.* (Ref. 6) found that their data were consistent with an energy defect of about 0.2 eV.

[38]W. B. Maier II, Los Alamos Scientific Laboratory Report No. LA-3972, 1969 (unpublished).

[39]W. B. Maier II, J. Chem. Phys. 41, 2174 (1964).

[40]Here the distinction between crossings and pseudocrossings of potential energy curves is ignored. See Ref. 2, p. 440.

[41]B. L. Moiseiwitsch, J. Atmospheric Terrest. Phys. Special Suppl. 2, 23 (1955). His $I(\eta)$ is the present $J(\xi)$.

[42]See Ref. 2, p. 444; or J. L. Magee, Discussions Faraday Soc. 12, 33 (1952).

[43]Lawrence Willets, in *Proceedings of the Second International Conference on the Physics of Electronic and Atomic Collisions, Abstracts of Papers* (Benjamin, New York, 1961), p. 47.

[44]J. L. Franklin, J. G. Dillard, H. M. Rosenstock, J. T. Herron, K. Draxl, and F. H. Field, Natl. Bur. Std. (U. S.) Ref. Data Ser. No. 26 (U. S. GPO, Washington, D. C., 1969).

[45]C. E. Moore, Natl. Bur. Std. Circ. No. 467, (U. S. GPO, Washington, D. C., 1952), Vol. II.

[46]Naturally, this statement depends on the angular distribution of secondary ions in the c.m. system. Two fairly reasonable examples are given in Ref. 38 for reactions of the sort $A^+ + B \rightarrow B^+ + A$.

[47]Reactions which produce a free electron probably produce more forwardly directed secondary ions than the other reactions, even for the same value of γ. See Ref. 38.

[48]If the secondary ions are scattered isotropically in the laboratory, then K_2 should be about 15. For $Kr^{++} + Ne \rightarrow Ne^+$, the measured value of K_2 is >9.

[49]See Ref. 18, Fig. 2, for an example.

[50]The cross section for $N_2^+ + N_2 \rightarrow N_2 + N_2^+$ is in very good agreement with the same cross section measured by J. J. Leventhal, T. F. Moran, and L. Friedman, J. Chem. Phys. 46, 4666 (1967).

[51]See Ref. 1, p. 662ff; the factor f is not in Eq. (101) on p. 663, but is in Eq. (107) on p. 667. See also Ref. 41. Particular states of A^+ and B may give rise to several electronic states of the AB^+ molecule. f is the probability that the colliding atoms A^+ and B approach each other along an A^+B potential curve (Ref. 36) which crosses an appropriate potential curve for B^+A at a point such that dissociation into B^+ and A is possible.

[52]It is here assumed that $(l+\frac{1}{2})^2/R^2 = 0$ when $l = 0$ and that $x = \infty$ when $l = L$; compare Eqs. (101) and (108) in Chap. XIX of Ref. 1.

PHYSICAL REVIEW A VOLUME 5, NUMBER 3 MARCH 1972

Electronic Transitions in Slow Collisions of Atoms and Molecules. IV. Multistate Eikonal Approximation for Quasiadiabatic Transitions*

Joseph C. Y. Chen
Department of Physics and Institute for Pure and Applied Physical Sciences, University of California, San Diego, La Jolla, California 92037
and
Charles J. Joachain† and Kenneth M. Watson
Department of Physics and Lawrence Radiation Laboratory, University of California, Berkeley, California 94720
(Received 26 July 1971)

The coupled equations of the adiabatic-state expansion method for quasiadiabatic transitions in atomic collisions are reduced in the eikonal approximations to a form that allows straightforward computation. The multistate eikonal approximation is then applied to the $He^+(1s) + H(1s) \rightarrow He^+(1s) + H(2p)$ excitation process. The partial and total $2p$-excitation cross sections as well as the polarization of the light emitted by the excited H atoms are calculated. Our results compare well with recent experimental measurements. The importance of final-state coupling is dramatically illustrated by the above $2p$-excitation process. The qualitative features of the nonadiabatic effects are also investigated in the eikonal Born approximation as functions of the position and distance of closest approach of the two adiabatic states.

I. INTRODUCTION

In Paper I of this series,[1] the adiabatic-state expansion method for atomic scattering and rearrangement collisions was critically examined. Several difficulties and ambiguities for rearrangement collisions were resolved. It was then shown that the use of the eikonal approximation to describe the motion of the atoms or ions or both permits the coupled equations of the adiabatic-state expansion method to be reduced to one-dimensional equations defined along classical trajectories. Several practical techniques for evaluating wave functions and Green's functions in the eikonal approximation were introduced in Paper II.[2] A variational technique based on the "principle of least action" was also developed in Paper II for the calculation of the trajectory. Numerical illustrations of these various techniques were carried out for the (H^+, H) and (He^+, He) collision systems in both the classical limit and the nonclassical regime of the eikonal approximation.[2,3] In all these applications, we were dealing essentially with potential-scattering problems. In the present paper we shall consider the problem of quasiadiabatic transitions in the multistate eikonal approximation.

The eikonal approximation will be valid if (in the notation of Paper I)

$$\eta_3 \equiv \hbar/pa_0 \ll 1 , \tag{1.1}$$

where p is the relative momentum of the colliding particles. Our approximation scheme is expected to converge rapidly if the adiabatic criterion is met:

$$\eta_2 = v/(e^2/\hbar) \ll 1 . \tag{1.2}$$

Let E be the initial kinetic energy (in a.u.) of the colliding particles in the c.m. system. We shall assume conditions (1.1) and (1.2) and, further, that

$$E \gg 1 , \tag{1.3}$$

which permits us (see Paper II) to calculate the eikonal with the approximation that the trajectories lie along straight lines. When condition (1.3) is met, the eikonal criterion [Eq. (1.1)] will always be satisfied.

In the adiabatic-state expansion method, the state function ψ_a^+ is represented by the expansion [see Eqs. (I2.14) and (I3.20)]